

The G₀/G₁ Switch Gene 2 Regulates Adipose Lipolysis through Association with Adipose Triglyceride Lipase

Xingyuan Yang,^{1,2} Xin Lu,^{1,2} Marc Lombès,⁵ Geun Bae Rha,^{3,4} Young-In Chi,^{3,4} Theresa M. Guerin,^{1,2} Eric J. Smart,^{1,2} and Jun Liu^{1,2,*}

¹Department of Pediatrics

²Kentucky Pediatric Research Institute

³Department of Molecular and Cellular Biochemistry

⁴Center for Structural Biology

University of Kentucky, Lexington, KY, USA

⁵Inserm U693, Faculté de Médecine Paris-Sud, Le Kremlin Bicetre, France

*Correspondence: jun.liu@uky.edu

DOI 10.1016/j.cmet.2010.02.003

SUMMARY

Adipose triglyceride lipase (ATGL) is the rate-limiting enzyme for triacylglycerol (TAG) hydrolysis in adipocytes. The precise mechanisms whereby ATGL is regulated remain uncertain. Here, we demonstrate that a protein encoded by G₀/G₁ switch gene 2 (G0S2) is a selective regulator of ATGL. G0S2 is highly expressed in adipose tissue and differentiated adipocytes. When overexpressed in HeLa cells, G0S2 localizes to lipid droplets and prevents their degradation mediated by ATGL. Moreover, G0S2 specifically interacts with ATGL through the hydrophobic domain of G0S2 and the patatin-like domain of ATGL. More importantly, interaction with G0S2 inhibits ATGL TAG hydrolase activity. Knockdown of endogenous G0S2 accelerates basal and stimulated lipolysis in adipocytes, whereas overexpression of G0S2 diminishes the rate of lipolysis in both adipocytes and adipose tissue explants. Thus, G0S2 functions to attenuate ATGL action both *in vitro* and *in vivo* and by this mechanism regulates TAG hydrolysis.

INTRODUCTION

During instances of heightened metabolic demand, triacylglycerol (TAG) stores in lipid droplets of adipocytes undergo a hydrolytic process (lipolysis) to release free fatty acids (FFAs) and glycerol into the circulation for use by other organs (Duncan et al., 2007). The regulation of lipolysis in adipocytes has been well studied for nearly half a century, with most of the attention focused on hormone-sensitive lipase. In a well-established model, the cAMP-dependent protein kinase (PKA) phosphorylates hormone-sensitive lipase (HSL) and the lipid droplet coat protein perilipin A in response to β -adrenergic hormones. Consequently, HSL translocates from the cytoplasm onto lipid

droplets, thereby mediating TAG hydrolysis (Egan et al., 1992; Sztalryd et al., 2003). However, the failure of HSL null mice to display an obese phenotype led to the discovery of an independent TAG hydrolase named adipose triglyceride lipase (ATGL) (Jenkins et al., 2004; Villena et al., 2004; Zimmermann et al., 2004). The complete lipolysis in adipocytes is delicately regulated and is now believed to be catalyzed sequentially by ATGL, HSL, and monoacylglycerol (MAG) lipase (Raben and Baldassare, 2005; Watt and Steinberg, 2008; Zechner et al., 2009; Zimmermann et al., 2009).

ATGL is highly expressed in adipose tissue (Villena et al., 2004; Zimmermann et al., 2004). Its TAG hydrolase activity is dependent on a "patatin domain" common to plant acyl-transferases (Dessen et al., 1999; Rydel et al., 2003). Analysis using cultured cells demonstrated that ATGL was involved in basal and hormone-stimulated lipolysis in adipocytes (Bezaire et al., 2009; Kershaw et al., 2006; Zimmermann et al., 2004) and lipid droplet degradation in nonadipocyte cells (Smirnova et al., 2006). Most notably, ATGL null mice showed impaired lipolysis in adipocytes in response to β -adrenergic stimulation accompanied by an expanded adipose tissue mass and increased TAG deposition in most other tissues (Haemmerle et al., 2006). Exercise-induced lipolysis was also shown to be blunted in these mice (Huijsman et al., 2009). Conversely, adipose-specific overexpression of ATGL promoted lipolysis and attenuated diet-induced obesity in mice (Ahmadian et al., 2009). In humans, a subgroup of neutral lipid storage disease (NLS) characterized by mild myopathy was reported to be caused by mutations in ATGL (Fischer et al., 2007). Although experiments using a specific HSL inhibitor and siRNA-mediated knockdown of ATGL suggested that HSL might be more important in mediating hormone-stimulated lipolysis in human fat (Langin et al., 2005; Rydén et al., 2007), a very recent study provided evidence that, in human adipose tissue-derived multipotent stem cell (hMADS) adipocytes, ATGL acted independently of HSL and preceded its action in the sequential hydrolysis of TAG (Bezaire et al., 2009). Collectively, these studies have provided compelling evidence to establish ATGL as the key enzyme catalyzing adipocyte lipolysis.

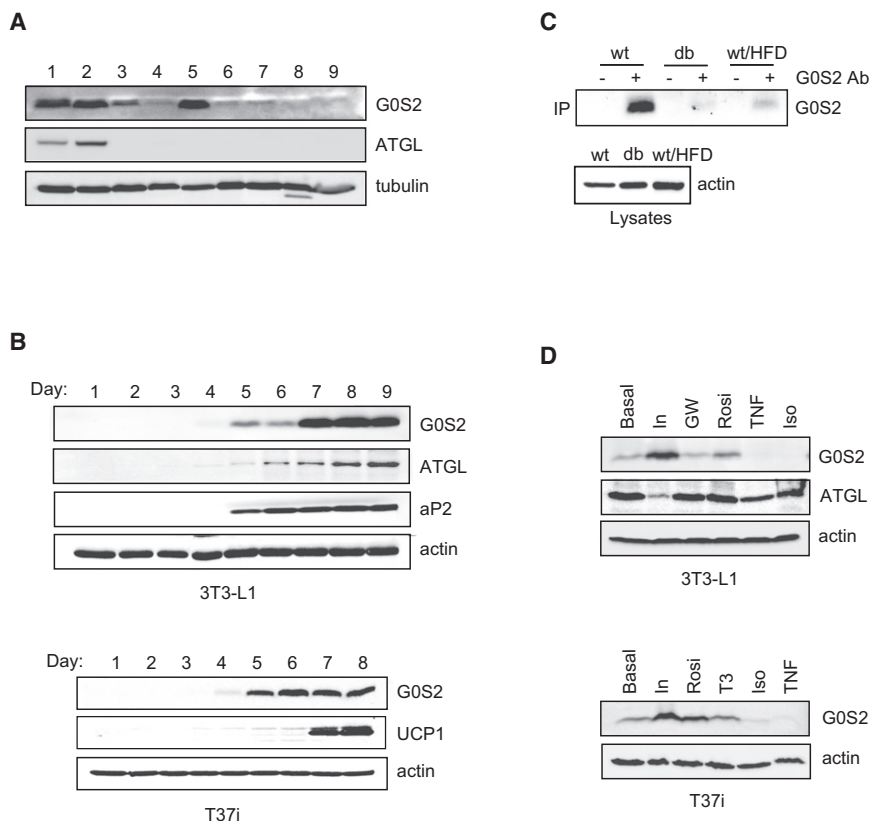


Figure 1. Regulation of G0S2 Protein Expression

(A) Tissue distribution of G0S2 protein by immunoblotting analysis. 1, epididymal white adipose tissue; 2, interscapular brown adipose tissue; 3, heart; 4, skeletal muscle (hindlimb, upper-leg muscle); 5, liver; 6, lung; 7, spleen; 8, pancreas; 9, kidney. β -tubulin was used as a loading control. (B) Expression of G0S2 protein was analyzed by immunoblotting in lysates from differentiated 3T3-L1 and T37i adipocytes. Day 1 represents undifferentiated preadipocytes. aP2 was used as an adipocytes differentiation marker. UCP1 was used as a brown adipocyte specific marker. β -actin was used as a loading control.

(C) Immunoprecipitation was performed in extracts (equal amount of total protein) of mouse epididymal adipose using either anti-G0S2 serum (+) or preimmune serum (-). G0S2 in the immunoprecipitates were analyzed by immunoblotting. Mice used are wild-type mice (wt) and *db/db* mice on normal chow and wild-type mice fed with high-fat diet for 8 weeks (wt/HFD).

(D) Following 4 hr serum deprivation, 3T3-L1 and T37i adipocytes were treated for 8 hr with 50 nM insulin (In), 10 nM triiodothyronine (T3), 10 μ M GW501516 (GW), 1 μ M rosiglitazone (Rosi), 1 μ M isoproterenol/0.25 mM IBMX (Iso) or 20 ng/ml TNF α in serum-free medium. Immunoblotting was performed to detect the levels of G0S2 in the cell lysates, using β -actin as a loading control.

In contrast to HSL, relatively little is known about the mechanisms whereby ATGL activity is regulated. Lass et al. demonstrated that comparative gene identification-58 (CGI-58) stimulates lipolysis and is an activator of ATGL, but not HSL (Lass et al., 2006). Earlier studies identified mutations in the human CGI-58 gene as a cause for Chanarin-Dorfman syndrome (CDS), a rare form of NLSO characterized by ichthyosis (Lefèvre et al., 2001). Of interest, CGI-58 mutants associated with CDS failed to activate ATGL (Lass et al., 2006), implying that loss of ATGL activation may be involved in the pathogenesis of CDS. Moreover, ATGL was shown to interact physically with pigment epithelium-derived factor (PEDF) in liver (Chung et al., 2008; Notari et al., 2006). PEDF-deficient hepatocytes exhibited increased TAG accumulation, suggesting that PEDF also plays a positive role in regulating ATGL-mediated lipolysis. Furthermore, ATGL activity in adipocytes is known to be promoted by β -adrenergic stimulation (Haemmerle et al., 2006; Zimmermann et al., 2009). Although PKA does not appear to directly phosphorylate ATGL (Zimmermann et al., 2004), recent work by Miyoshi et al. demonstrated that phosphorylation of Ser517 in perilipin A was essential for activation of ATGL in vivo (Miyoshi et al., 2007).

Here, we demonstrate that G_0/G_1 switch gene 2 (G0S2), a protein whose function was previously unclear, is, in fact, a negative regulator of ATGL. G0S2 was originally identified in blood mononuclear cells due to the association of its mRNA expression with re-entry of cells from G_0 into G_1 phase (Russell and Forsdyke, 1991). However, its role in cell-cycle regulation has never been established. Zandbergen et al. later reported

that the G0S2 mRNA level was highest in adipose tissue and was upregulated during adipogenic differentiation of preadipocytes (Zandbergen et al., 2005). In this study, we performed functional analysis of G0S2 by using a variety of in vitro and cell-based approaches. Our results indicate that G0S2 binds directly to ATGL and is capable of attenuating ATGL-mediated lipolysis via inhibiting its TAG hydrolase activity.

RESULTS

Expression Pattern of G0S2 Protein

To initiate functional studies, we raised antibodies against murine G0S2 (Figure S1 available online) and determined its expression pattern. Immunoblotting of various mouse tissues demonstrated an abundant expression of G0S2 in white and brown adipose tissues (WAT and BAT) and liver and, to a lesser degree, in heart (Figure 1A). The adipose-specific expression of G0S2 was corroborated in mouse white 3T3-L1 and brown T37i preadipocyte cell lines (Figure 1B). In both cell types, G0S2 protein expression was first detected 4 days after adipogenic induction. The maximal level was reached after 7 days, when 3T3-L1 cells were fully differentiated, as judged by expression of an adipocyte marker aP2. In T37i cells, the G0S2 expression became robust after 5 days. UCP1, a brown adipocyte-specific mitochondrial marker, appeared at the 7 day time point. These results indicate a differentiation-dependent expression of G0S2 protein in adipocytes. In mouse WAT, amounts of G0S2 were significantly decreased in *db/db* mice compared with that of wild-type mice (Figure 1C). Chronic high-fat feeding of

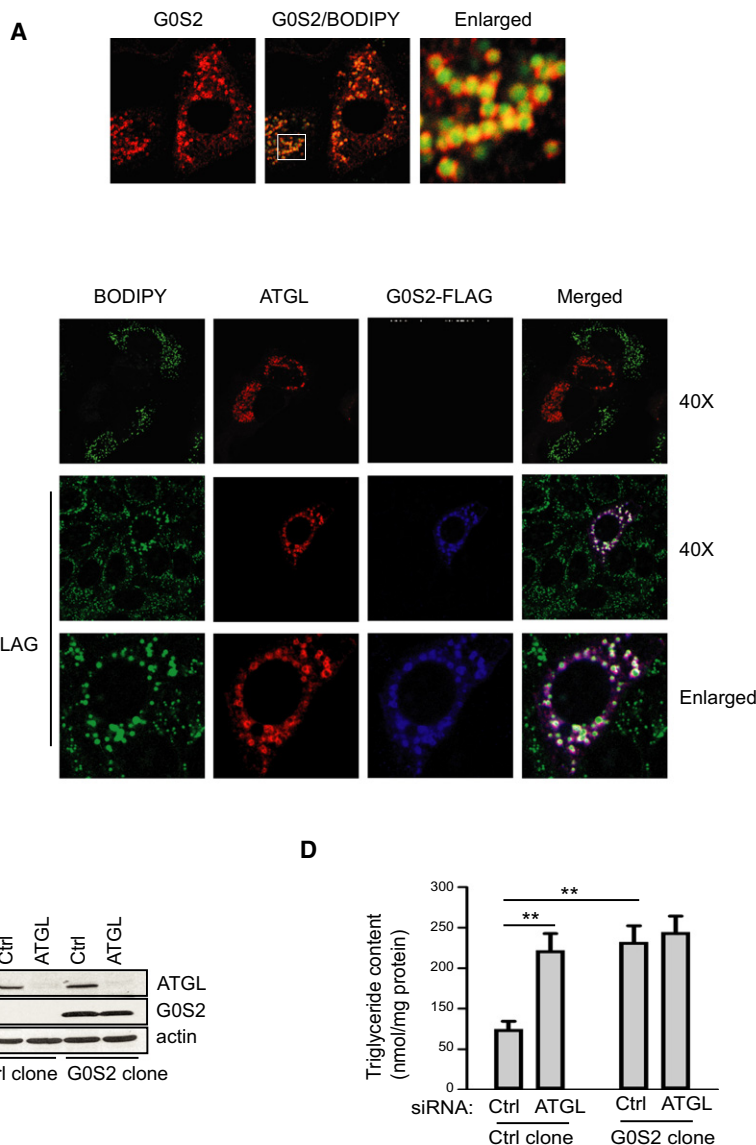


Figure 2. G0S2 Inhibits Lipid Droplet Degradation Mediated by ATGL

(A) Immunofluorescence staining with anti-G0S2 antibodies was performed to reveal localization of overexpressed untagged G0S2 in HeLa cells. Lipid droplets were costained with BODIPY 493/503 fluorescence dye.

(B) HeLa cells transfected with ATGL in the absence (top) or presence (bottom) of G0S2-FLAG were incubated under normal growth conditions with 400 μ M of oleic acid complexed to albumin for 3 hr. Immunofluorescence staining was performed by using anti-ATGL (red) and anti-FLAG (blue) antibodies. Lipid droplets were costained with BODIPY 493/503 fluorescence dye.

(C and D) Stable HeLa cell clones with or without untagged G0S2 expression were treated with ATGL siRNA (ATGL KD) or control mismatch siRNA (Ctrl KD). Protein expression was analyzed by immunoblotting with anti-ATGL and anti-G0S2 antibodies (C). The cells were incubated in 400 μ M of oleic acid for 3 hr, and the intracellular TAG content was determined as described in [Experimental Procedures](#). The data were normalized with the total protein amounts in the cell extracts (D).

Data are shown as mean \pm SD and represent three independent experiments. ** p < 0.01, t test.

wild-type mice also reduced the level of G0S2 in WAT, suggesting that G0S2 expression negatively correlates with the development of obesity.

Treatment with insulin profoundly increased G0S2 expression in both 3T3-L1 and T37i adipocytes (Figure 1D). Conversely, prolonged treatment with β -adrenergic agonist isoproterenol or another lipolysis-inducing hormone $\text{TNF}\alpha$ drastically decreased G0S2 level in both cell types. Moreover, no effects were observed when adipocytes were treated with GW501516 (a PPAR δ ligand) or T3 (thyroid hormone). Rosiglitazone, however, significantly enhanced G0S2 expression in both cell types, confirming that G0S2 is a PPAR γ downstream target (Zandbergen et al., 2005).

G0S2 Prevents Lipid Droplet Turnover Mediated by ATGL

To obtain further insight into the potential function of G0S2, we expressed G0S2 in HeLa cells and determined its subcellular

localization by immunofluorescence staining. As shown in Figure 2A, G0S2 displayed a pattern of small rings that scattered throughout the cytoplasm. Using BODIPY 493/503, a nonpolar probe selective for neural lipids such as TAG, we identified that these ring-like structures surrounded the central cores of lipid droplets. Because lipid droplets undergo constant synthesis and turnover (Martin and Parton, 2006), we next examined the potential involvement of G0S2 in regulating lipid droplet stability. HeLa

cells transiently expressing G0S2 were treated with oleic acid for 3 hr to promote lipid droplet formation (Figure S2A). Lipid droplets in cells expressing G0S2 were significantly larger and more numerous than those in the neighboring untransfected cells (Figure S2A, top). Overloading the cells with oleic acid for 24 hr resulted in accumulation of large lipid droplets in both transfected and untransfected cells, with no obvious difference in size and number (Figure S2A, middle). However, after 24 hr of oleic acid treatment followed by nutrient starvation for 4 hr, lipid droplets in untransfected cells underwent pronounced degradation while overexpression of G0S2 was able to prevent such turnover (Figure S2A, bottom). For the three experimental conditions employed, the average diameter of lipid droplets in untransfected cells versus G0S2-transfected cells was 0.45 μ m versus 0.89 μ m, 1.13 μ m versus 1.22 μ m, and 0.34 μ m versus 0.99 μ m, respectively (Figure S2B).

Because ATGL plays a key role in lipid droplet degradation in HeLa cells (Smirnova et al., 2006), we tested whether G0S2

would neutralize this effect of ATGL action. Upon oleic acid loading, HeLa cells transfected with ATGL alone showed a marked reduction in both size and number of lipid droplets compared with the adjacent untransfected controls (Figure 2B, top). Interestingly, coexpression of G0S2 tagged at the C terminus with a FLAG epitope (G0S2-FLAG) was able to reverse this effect of ATGL overexpression (Figure 2B, middle). Consequently, G0S2-FLAG and ATGL were found to be colocalized at the surface of lipid droplets (Figure 2B, bottom). To further assess whether G0S2 and ATGL, singly or in combination, affect intracellular TAG accumulation, we generated HeLa cells stably expressing untagged G0S2 and then employed siRNA to knock down ATGL in these cells. The knockdown was equally effective at reducing endogenous ATGL in both G0S2-expressing and nonexpressing cells (Figure 2C). Less than 5% of ATGL was present in cells transfected with a pool of siRNAs directed against ATGL compared with cells transfected with a mismatched control siRNA. The TAG content in G0S2-expressing cells was profoundly increased upon oleic acid treatment compared with that in nonexpressing control cells (Figure 2D). Knockdown of ATGL promoted TAG accumulation in control cells, presumably due to decreased TAG hydrolysis. Strikingly, the effects of reduced ATGL expression and G0S2 overexpression are not additive because ATGL knockdown failed to further increase the TAG content in G0S2-expressing cells (Figure 2D). Taken together, these results suggest that G0S2 expression may stabilize lipid droplets and promote TAG accumulation via inhibiting ATGL-catalyzed lipolysis.

G0S2 Inhibits TAG Hydrolase Activity of ATGL

Murine G0S2 is a 103 amino acid protein with a central putative hydrophobic domain (residues 27–42) (Zandbergen et al., 2005). ATGL, on the other hand, belongs to a family of lipases containing a patatin domain essential for their hydrolase activity (Watt and Steinberg, 2008; Zimmermann et al., 2009). The C-terminal region of ATGL contains a putative lipid-binding domain that is highly hydrophobic (Fischer et al., 2007; Kobayashi et al., 2008; Schweiger et al., 2008) (Figure 3A). To determine whether G0S2 could regulate TAG hydrolase activity of ATGL, we transfected ATGL in G0S2-expressing or nonexpressing HeLa cells (Figure 3B). In assays with lysates of nonexpressing control cells, transfection of ATGL resulted in a > 4-fold increase in the TAG hydrolase activity when compared to transfection of vector alone. By contrast, overexpression of ATGL in G0S2-expressing cells failed to significantly enhance the lipase activity. G0S2 also significantly reduced the activity of ATGL Δ HD, a mutant that lacks the putative lipid-binding hydrophobic domain (Figure 3B). As a control, expression of HSL increased lipase activity by ~10-fold independently of G0S2 expression (Figure S3). Therefore, the presence of G0S2 substantially inhibits the enzymatic activity of ATGL, but not that of HSL.

Because ATGL is activated by CGI-58 (Lass et al., 2006), we investigated whether G0S2 could affect the TAG hydrolase activity of ATGL in the presence of CGI-58. To this end, ATGL, CGI-58, and G0S2 were expressed singly in HeLa cells, and then the TAG hydrolase activity was measured in combined cell extracts (Figure 3C). The addition of CGI-58-containing extracts to ATGL-containing extracts caused an ~4-fold increase in the TAG hydrolase activity. However, the further

addition of G0S2-containing extracts to the mixture considerably eliminated this activating effect of CGI-58, indicating that G0S2 is capable of inhibiting ATGL even in the presence of CGI-58. Similar results were obtained by adding recombinant G0S2 protein expressed and purified from *E. coli* to ATGL and CGI-58 produced from an in vitro transcription/translation system. As shown in Figure 3D, purified G0S2 dose dependently inhibited the TAG hydrolase activity of ATGL in both the absence and presence of CGI-58. Moreover, varying amounts of purified G0S2 were added to mouse WAT and BAT extracts, with the highest concentration decreasing their total TAG hydrolase activity by 32% and 38%, respectively (Figure 3E). The differences are significant considering that, although ATGL is the main TAG hydrolase in vivo, a large portion of the total in vitro activity toward TAG substrate is accounted for by HSL and therefore may not be affected by G0S2.

G0S2 Directly Interacts with ATGL

To determine whether G0S2 physically interacts with ATGL, we transiently expressed ATGL and G0S2-FLAG in HeLa cells and evaluated their interaction by coimmunoprecipitation assays (Figure 4A). As revealed by immunoblotting of total proteins from cell lysates, comparable levels of ATGL were expressed with or without G0S2-FLAG. Anti-FLAG immunoprecipitation demonstrated a specific association of ATGL with precipitated G0S2-FLAG. To identify the structural determinants required for the G0S2-ATGL interaction, we generated several deletion mutants of G0S2 and ATGL (Figure 3A). Whereas G0S2₁₋₇₃ contains the N-terminal 73 amino acids including an intact hydrophobic domain, G0S2 Δ HD is an internal deletion mutant lacking the hydrophobic domain. Meanwhile, ATGL Δ PT and ATGL Δ HD are two internal deletion mutants that lack the patatin domain (residues 10–178) and the hydrophobic domain (residues 259–337), respectively. As shown in Figure 4A, G0S2-FLAG coimmunoprecipitated with both wild-type ATGL and ATGL Δ HD mutant, whereas ATGL Δ PT mutant exhibited no interaction with G0S2-FLAG. In a separate experiment, G0S2₁₋₇₃-FLAG was found to interact with ATGL with the same affinity as the full-length G0S2-FLAG. However, G0S2 Δ HD-FLAG showed no binding to ATGL (Figure 4B). Therefore, the hydrophobic domain in G0S2 and the patatin domain of ATGL are needed for mediating the specific association.

To determine whether interaction occurs between the endogenous proteins, ATGL was immunoprecipitated from 3T3-L1 adipocyte lysates with anti-ATGL antibodies. As controls, immunoprecipitation was performed using nonspecific or anti-HSL antibodies, as well as using ATGL antibodies in the presence of an ATGL-blocking peptide. As shown in Figure 4C, endogenous ATGL and HSL were efficiently pulled down by respective antibodies. G0S2 was specifically coimmunoprecipitated with ATGL, but not with HSL. The blocking peptide was able to abolish both immunoprecipitation of ATGL and coimmunoprecipitation of G0S2 by ATGL antibodies, demonstrating the specificity of their association. The complex formation appears to be stable because pretreatment of cells with either isoproterenol or insulin conferred no significant impact on the G0S2-ATGL coimmunoprecipitation (Figure 4C).

To exclude the possibility that the complex formation is bridged by a third protein in cells, we assayed the interaction

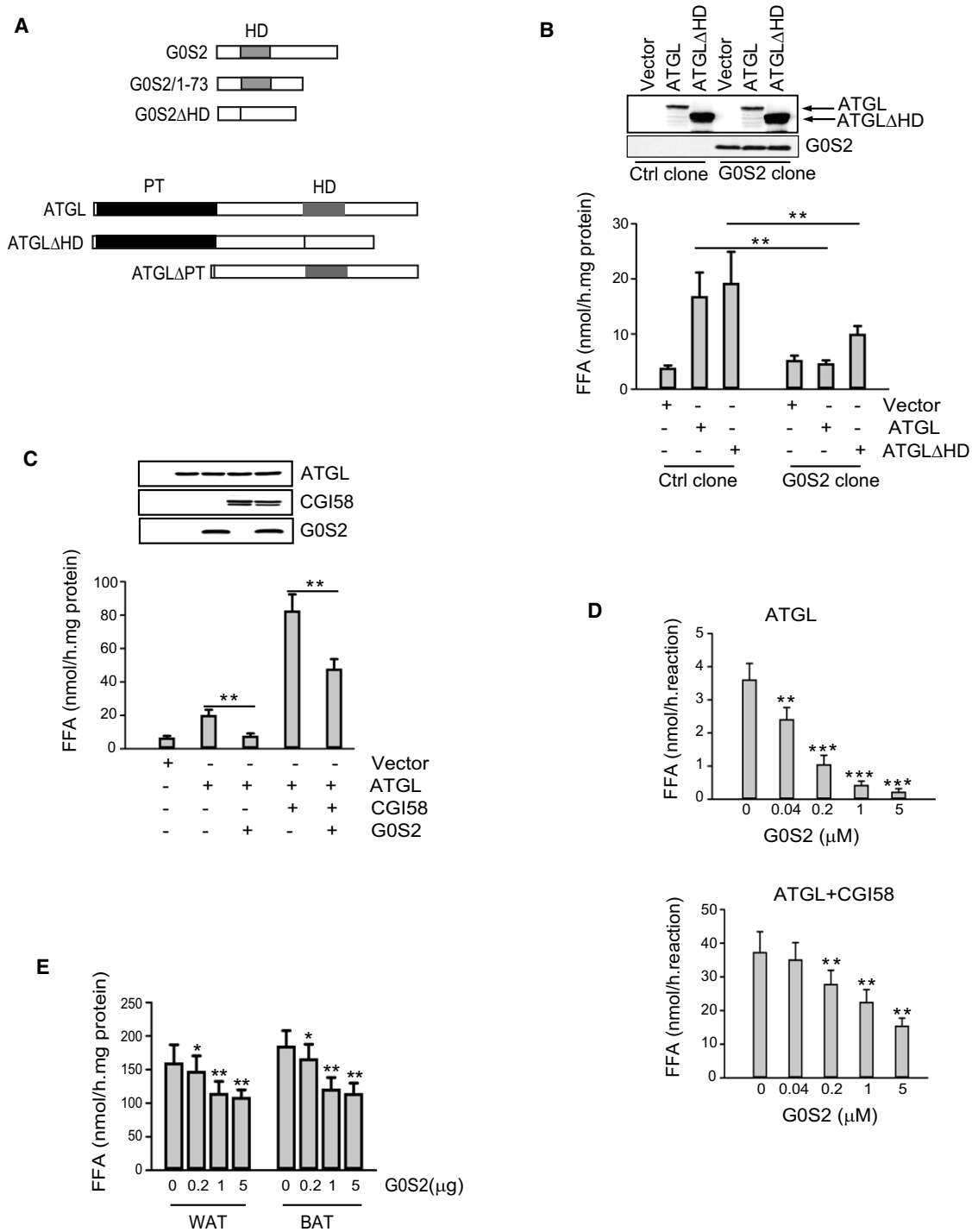


Figure 3. G0S2 Selectively Inhibits the TAG Hydrolase Activity of ATGL

(A) Schematic structures of generated mutants of murine G0S2 and ATGL. The location of the hydrophobic domain (HD) in both proteins is indicated as gray bars, and the patatin domain (PT) in ATGL is indicated by a black region.

(B) HeLa cells from control clone or G0S2-expressing clone were transfected with vector alone, ATGL, and ATGLΔHD. At 24 hr after transfection, ATGL and G0S2 proteins were detected with anti-ATGL and anti-G0S2 antibodies in immunoblotting using cell extracts. TAG hydrolase activity in cell extracts was measured using ³H-labeled triolein as substrate and was normalized with the total protein levels of the cell extracts.

(C) Extracts of HeLa cells singly expressing ATGL, CGI-58, or G0S2 were mixed in various combinations, and TAG hydrolase activity was determined. Proteins in parallel mixtures were revealed in immunoblotting.

(D) ATGL and CGI-58 produced by using *in vitro* translation system were mixed with increasing amounts of purified recombinant G0S2 and were subjected to TAG hydrolase activity assays.

between G0S2 and ATGL proteins produced by in vitro transcription/translation system (Figure 4D). As expected, ATGL was coimmunoprecipitated with G0S2-FLAG when they were present in the same reaction, demonstrating a direct association in vitro. The association with ATGL required the hydrophobic domain of G0S2 because ATGL did not coprecipitate with an internal deletion mutant of G0S2 (G0S2 Δ HD-FLAG) (Figure 4D). In addition, we analyzed the TAG hydrolase activity in reaction mixtures containing ATGL with wild-type G0S2-FLAG or G0S2 Δ HD-FLAG (Figure 4E). G0S2-FLAG decreased the TAG hydrolase activity in ATGL-containing mixture by ~70%, whereas G0S2 Δ HD-FLAG had no significant effect, indicating that direct interaction is necessary for efficient inhibition of ATGL by G0S2.

Lipid Droplet Localization of G0S2 in Adipocytes Depends on Interaction with ATGL

ATGL activity in vivo is determined by its lipid droplet localization (Fischer et al., 2007; Kobayashi et al., 2008; Schweiger et al., 2008). To analyze the relative localization of endogenous ATGL and G0S2, we performed lipid droplet fractionation experiments using 3T3-L1 adipocytes (Figure 5A). In basal state, only low levels of HSL, ATGL, and G0S2 were detected in the association with lipid droplets. Insulin treatment mildly increased the amounts of ATGL and G0S2, but not HSL, in the lipid droplet fraction. As expected, stimulation of lipolysis with isoproterenol promoted translocation of HSL to lipid droplet fraction where upward shift of perilipin was also observed due to PKA phosphorylation. Of interest, isoproterenol also caused a marked movement of both ATGL and G0S2 to lipid droplets (Figure 5A). A time course experiment showed a rapid and sustained accumulation of ATGL and G0S2 in lipid droplets over the course of 10–120 min poststimulation (Figure S4). Lipid droplet translocation of ATGL and G0S2 was independently confirmed by immunofluorescence microscopy, as isoproterenol caused redistribution of ATGL and G0S2 staining from cytoplasm to rim-like structures surrounding lipid droplets (Figure 5B). To determine whether G0S2 moves onto lipid droplets in a complex with ATGL, we tested the effect of ATGL knockdown on the lipid droplets translocation of G0S2. As revealed by immunoblotting in Figure 5C, an ~90% knockdown efficiency was achieved by the combined usage of a pool of siRNAs against murine ATGL in comparison to mismatched controls. Of interest, knockdown of ATGL expression reduced the overall level of G0S2 protein while having no effect on the expression of HSL and perilipin. More importantly, G0S2 was absent in the lipid droplet fraction isolated from isoproterenol-treated cells transfected with ATGL siRNA (Figure 5C), suggesting that the lipid droplet localization of G0S2 may indeed depend on its interaction with ATGL.

G0S2 Attenuates Lipolysis in Adipocytes

The findings that G0S2 interacts with and inhibits ATGL prompted us to investigate the potential role of G0S2 in adipocyte lipolysis. To this end, we reduced the G0S2 level in 3T3-L1 adipocytes by siRNA-mediated knockdown. Compared with

mismatch control siRNA, the siRNA directed against G0S2 was effective at inhibiting G0S2 expression in 3T3-L1 adipocytes (Figure 6A). Importantly, lipolysis in 3T3-L1 cells was significantly enhanced by G0S2 knockdown in a time-dependent manner. After a 2 hr incubation period, basal and isoproterenol-stimulated FFA release was increased by 103% and 75%, respectively (Figure 6A). The effect of G0S2 knockdown on glycerol release followed the same trend, though it was less prominent (Figure 6A).

To corroborate our knockdown results, we performed gain-of-function studies by infecting adipocytes with an adenovirus encoding murine G0S2 (Ad-G0S2). Two different dosages of Ad-G0S2 and a null virus were employed, with the higher dose of Ad-G0S2 achieving a ~4-fold increase in G0S2 expression in 3T3-L1 adipocytes (Figure 6B). Infection of 3T3-L1 cells with Ad-G0S2 at this higher dosage significantly reduced basal and stimulated lipolysis when compared to infection with the null virus. In addition, infection of WAT explants with Ad-G0S2 virus inhibited isoproterenol-stimulated FFA release by ~40% (Figure 6C). However, ectopic expression of G0S2 in WAT explants only had a mild effect on basal FFA release. Nonetheless, these results collectively demonstrate a critical role of G0S2 in the control of adipose lipolysis.

DISCUSSION

As a closely controlled process essential for survival, lipolysis in adipocytes has been well studied for several decades. The discovery of ATGL as the key enzyme in adipocyte lipolysis is relatively recent (Zimmermann et al., 2009), and how ATGL activity is regulated is mostly unknown. The present study provides compelling evidence that G0S2 is an important negative regulator of ATGL-mediated lipolysis. Like ATGL (Figures 1A and 1B) (Villena et al., 2004; Zimmermann et al., 2004), G0S2 protein is highly expressed in adipose tissue, and its expression was induced during adipocyte differentiation. Biochemically, G0S2 binds directly to ATGL and is capable of inhibiting its TAG hydrolase activity. Functionally, overexpression of G0S2 prevents ATGL-mediated lipid droplet degradation in HeLa cells, as well as basal and stimulated lipolysis in cultured adipocytes and fat explants. Knockdown of endogenous G0S2, on the other hand, enhances adipocyte lipolysis under the same conditions.

G0S2 is a small basic protein with 78% identity between mouse and human isoforms. It has no homologs in lower organisms such as *Caenorhabditis elegans* and *Drosophila*. Our deletion mutagenesis experiments showed that the putative hydrophobic domain of G0S2 and the catalytic patatin-like domain of ATGL were responsible for mediating their specific interaction. Moreover, knockdown of ATGL decreased the overall content of G0S2 in adipocytes, indicating that intracellular stability of G0S2 may be enhanced by its interaction with ATGL. Although detailed structural studies are needed to delineate the possible mechanisms for inhibition of ATGL lipase activity by G0S2, we speculate that G0S2 binding may directly affect the substrate (TAG)

(E) Increasing amounts of recombinant purified G0S2 was added to extracts (100 μ g total protein) of epididymal (WAT) and interscapular (BAT) fat tissue, and TAG hydrolase activity was determined.

All data are shown as mean \pm SD and represent three independent experiments. * p < 0.05, ** p < 0.01, and *** p < 0.001, t test.

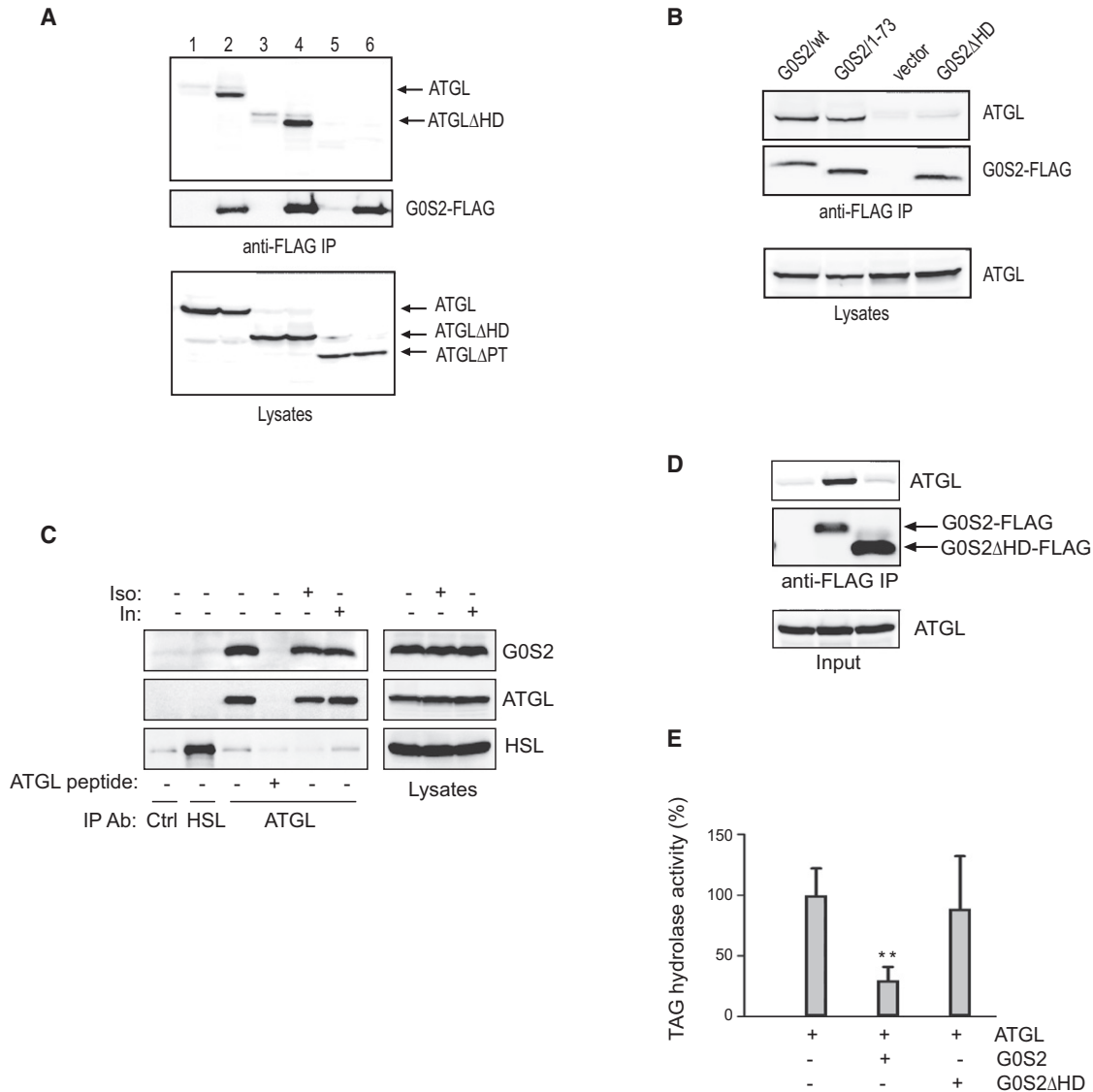


Figure 4. G0S2 Specifically Interacts with ATGL

(A) HeLa cells were cotransfected with vector alone or G0S2-FLAG together with different ATGL constructs (1, ATGL+vector; 2, ATGL+G0S2-FLAG; 3, ATGLΔHD+vector; 4, ATGLΔHD+G0S2-FLAG; 5, ATGLΔPT+vector; 6, ATGLΔPT+G0S2-FLAG). G0S2-FLAG proteins were immunoprecipitated with anti-FLAG antibodies. G0S2 and ATGL proteins in immunoprecipitates and lysates were detected by immunoblotting with FLAG and ATGL antibodies.

(B) HeLa cells were cotransfected with wild-type ATGL along with vector alone or various G0S2-FLAG constructs. Immunoprecipitation and immunoblotting analysis were performed as described in (A).

(C) 3T3-L1 adipocytes were pretreated with or without 1 μM isoproterenol or 100 nM insulin for 30 min. Immunoprecipitation of endogenous ATGL was performed in the lysates in the presence or absence of an ATGL epitope-blocking peptide. Nonspecific control and HSL antibodies were used as controls. G0S2, ATGL, and HSL in precipitates and lysates were analyzed by immunoblotting with respective antibodies.

(D) Anti-FLAG immunoprecipitation was performed following the in vitro transcription/translation reactions. ATGL and FLAG-tagged G0S2 proteins in precipitates were analyzed by immunoblotting with anti-ATGL and anti-FLAG antibodies.

(E) The TAG hydrolyase activity in the in vitro transcription/translation mixtures was measured using ³H-labeled triolein as substrate. The activity was normalized with the total protein levels of the reaction mixtures and is shown in relation to basal activity detected in reactions containing vector alone.

Data are shown as mean ± SD and represent three independent experiments. **p < 0.01, t test.

accessibility or simply alter the overall conformation of ATGL. Aside from being a TAG hydrolase, ATGL possesses activity as an acyl-CoA-independent transacylase, utilizing acylglycerols such as mono-olein or diolein as acyl donors/acceptors in the production of TAG (Jenkins et al., 2004). Therefore, it is also possible that the G0S2 binding can decrease the net fatty acid

release in a futile cycle by promoting ATGL-mediated transacylation of DAG and MAG back to TAG. Furthermore, we found that G0S2 was capable of dose dependently inhibiting ATGL even in the presence of the coactivator CGI-58, though CGI-58 rendered ATGL less sensitive to G0S2 inhibition. Because CGI-58 binds to the same N-terminal region of ATGL (Lass

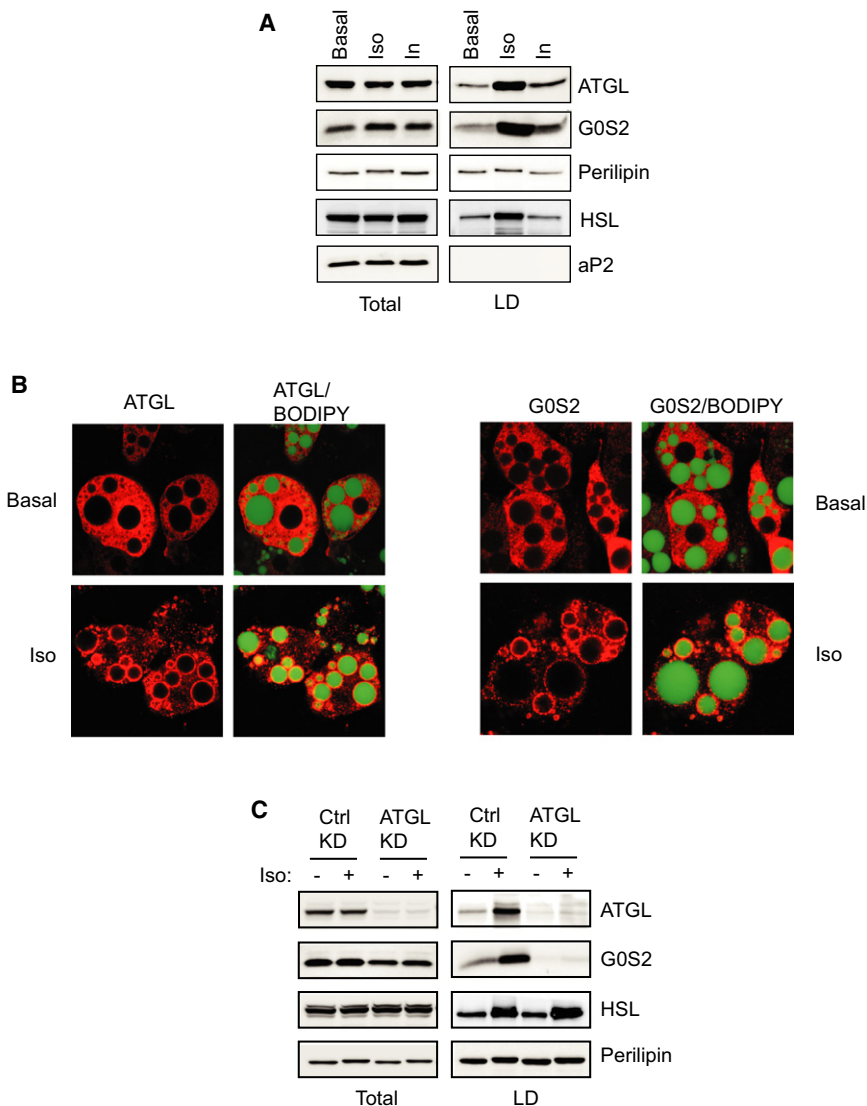


Figure 5. Lipid Droplet Localization of ATGL and G0S2 in Adipocytes

(A) 3T3 L1 adipocytes were treated with or without 1 μ M isoproterenol/0.25 mM IBMX or insulin for 30 min. Lipid droplets were isolated by ultracentrifugation. Total and lipid droplet-associated proteins were subjected to immunoblotting using antibodies against ATGL, perilipin, HSL, G0S2, and aP2.

(B) Immunofluorescence staining with anti-ATGL antibodies was performed to reveal localization of endogenous ATGL in 3T3-L1 adipocytes pre-treated with or without 1 μ M isoproterenol/0.25 mM IBMX for 30 min. Lipid droplets were costained with BODIPY 493/503.

(C) siRNA-mediated knockdown was performed by electroporating 3T3-L1 adipocytes with either control siRNA (Ctrl) or ATGL-specific siRNA (KD). Three days later, cells were treated with or without 1 μ M isoproterenol/0.25 mM IBMX for 30 min followed by lipid droplets isolation. Total and lipid droplet-associated levels of ATGL, HSL, G0S2, and perilipin were analyzed by immunoblotting.

ratio between G0S2 and ATGL levels may lead to lower lipolytic capacity and thus serve to facilitate the flow of fatty acid into TAG in WAT. During chronic exposure to starvation, catecholamines can turn off the expression of G0S2 as a way to sustain lipolysis in adipocytes.

By both lipid droplet fractionation and immunofluorescence staining, we demonstrated that isoproterenol treatment promoted rapid and dramatic translocation of ATGL from cytoplasm to the surface of lipid droplets. The observation that ATGL underwent HSL-like translocation to lipid droplets in response to lipolytic stimulation is potentially very important. The ATGL enzyme action, which is

dependent on its lipid droplet localization, is known to be sensitive to β -adrenergic stimulation in adipocytes (Zimmermann et al., 2009). However, unlike HSL, ATGL activity does not appear to be regulated directly by PKA phosphorylation (Zimmermann et al., 2004). Two previous studies demonstrated either a modest or no translocation of ATGL to lipid droplets in lipolytically stimulated cells (Granneman et al., 2007; Zimmermann et al., 2004). This discrepancy from our findings may be due to the fact that the previous experiments employed transient overexpression of epitope-tagged proteins, whereas our observations were made on endogenous ATGL. Similarly, Bezaire et al. showed that forskolin stimulated translocation of both HSL and ATGL to lipid droplets in human hMADs adipocytes (Bezaire et al., 2009). Together, these findings implicate a potential mechanism for the activation of ATGL in vivo in response to β -adrenergic stimulation. Of interest, Miyoshi et al. showed that ATGL action in adipocytes was controlled by PKA phosphorylation of Serine 517 of perilipin A (Miyoshi et al., 2007). Therefore, it would be tempting to examine whether this

et al., 2006; Schweiger et al., 2008), it would be interesting to determine whether CGI-58 and G0S2 directly compete with each other in the control of ATGL lipase activity. The expression of G0S2 is subject to hormonal and nutritional regulation. Previous studies have shown that G0S2 mRNA level is upregulated by insulin in skeletal muscle (Parikh et al., 2007), by glucose in liver (Ma et al., 2006), and by PPAR γ agonists in adipocytes (Zandbergen et al., 2005), indicating its role in energy metabolism. We found that G0S2 in adipocytes was reciprocally regulated by insulin and lipolytic stimulators. In contrast to reduced expression of ATGL (Figure 1D) (Kershaw et al., 2006), prolonged insulin treatment significantly upregulated G0S2 protein expression in adipocytes. Chronic treatment with isoproterenol and TNF α , on the other hand, drastically downregulated the level of G0S2. The fact that the expression of G0S2 as a lipolytic inhibitor can alter according to anabolic versus catabolic conditions implicates a potential mechanism to switch the balance between TAG mobilization and storage. In cases of caloric surplus, for example, an insulin-induced increase in the

dependent on its lipid droplet localization, is known to be sensitive to β -adrenergic stimulation in adipocytes (Zimmermann et al., 2009). However, unlike HSL, ATGL activity does not appear to be regulated directly by PKA phosphorylation (Zimmermann et al., 2004). Two previous studies demonstrated either a modest or no translocation of ATGL to lipid droplets in lipolytically stimulated cells (Granneman et al., 2007; Zimmermann et al., 2004). This discrepancy from our findings may be due to the fact that the previous experiments employed transient overexpression of epitope-tagged proteins, whereas our observations were made on endogenous ATGL. Similarly, Bezaire et al. showed that forskolin stimulated translocation of both HSL and ATGL to lipid droplets in human hMADs adipocytes (Bezaire et al., 2009). Together, these findings implicate a potential mechanism for the activation of ATGL in vivo in response to β -adrenergic stimulation. Of interest, Miyoshi et al. showed that ATGL action in adipocytes was controlled by PKA phosphorylation of Serine 517 of perilipin A (Miyoshi et al., 2007). Therefore, it would be tempting to examine whether this

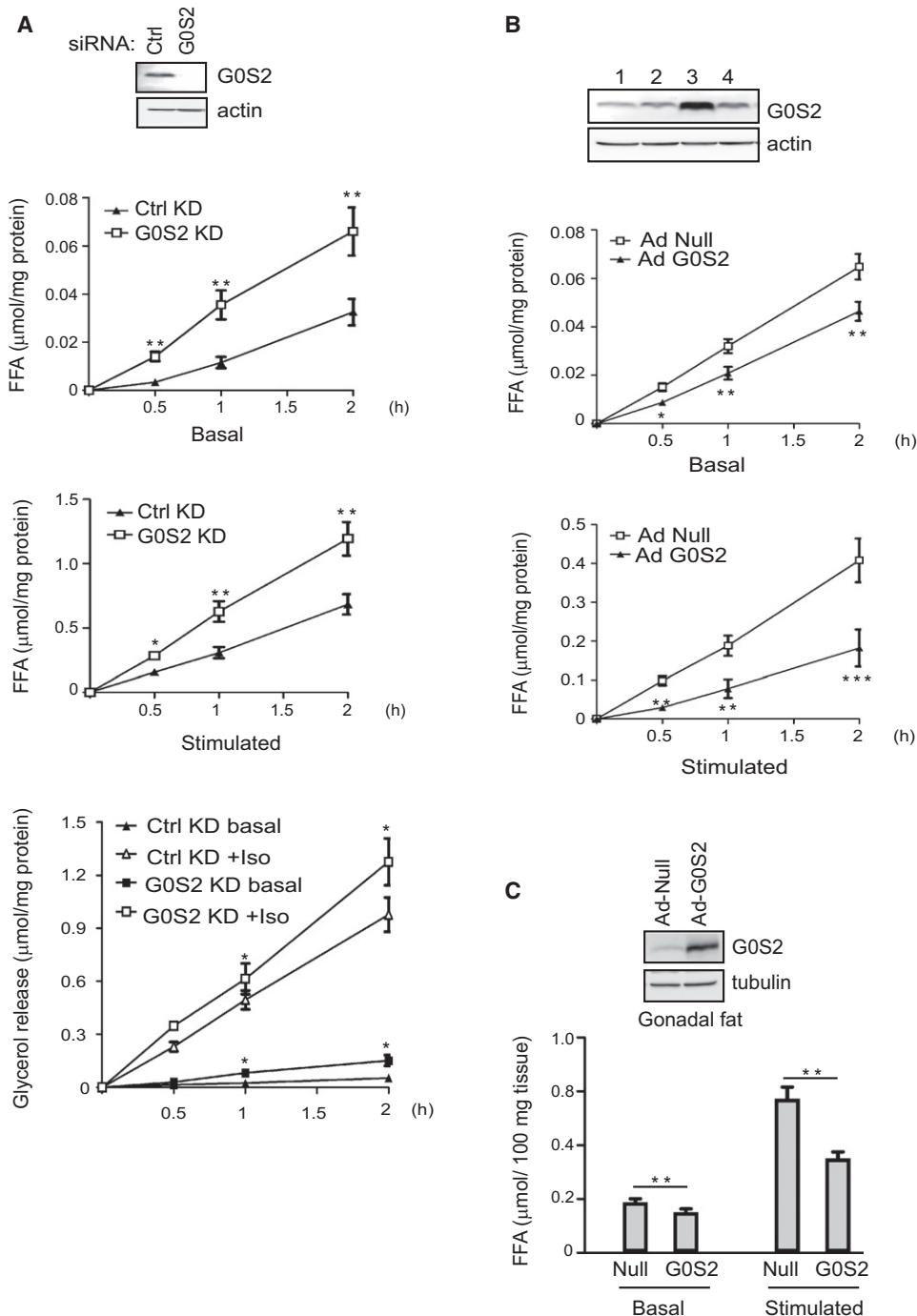


Figure 6. G0S2 Attenuates Basal and Stimulated Lipolysis in Adipocytes

(A) siRNA-mediated knockdown of G0S2 in 3T3-L1 adipocytes was achieved by electroporating cells with either control siRNA or G0S2-specific siRNA. Cells were treated 3 days later with (stimulated) or without (basal) $1 \mu\text{M}$ isoproterenol for 30 min, 60 min, and 2 hr. Basal and stimulated FFA and glycerol release were measured and normalized with the total protein levels in the cell extracts. Expression of G0S2 protein was analyzed by immunoblotting, using β -actin as a loading control. Data are shown as mean \pm SD and represent three independent experiments. * $p < 0.05$ and ** $p < 0.01$, one-way ANOVA.

(B) Overexpression of G0S2 in 3T3-L1 adipocytes was achieved by infecting cells with recombinant adenovirus encoding murine G0S2 (Ad-G0S2). A null virus was used as a control. G0S2 expression was analyzed by immunoblotting 3 days after infection. 1, null virus at high dosage; 2, null virus at low dosage; 3, Ad-G0S2 at high dosage; 4, Ad-G0S2 at low dosage. Three days following infection with either null or Ad-G0S2 at high dosage, lipolysis of 3T3-L1 adipocytes was measured as described in A. Data are shown as mean \pm SD and represent three independent experiments. * $p < 0.05$, ** $p < 0.01$, and *** $p < 0.001$, one-way ANOVA.

(C) Overexpression of G0S2 in gonadal fat explants was achieved by infection with Ad-G0S2 using null virus as a control. At 2 days postinfection, explants were treated with (stimulated) or without (basal) $1 \mu\text{M}$ isoproterenol for 2 hr. Basal and stimulated FFA release was measured and normalized with the total mass of explants. Data are shown as mean \pm SD and represent three independent experiments. ** $p < 0.01$, t test.

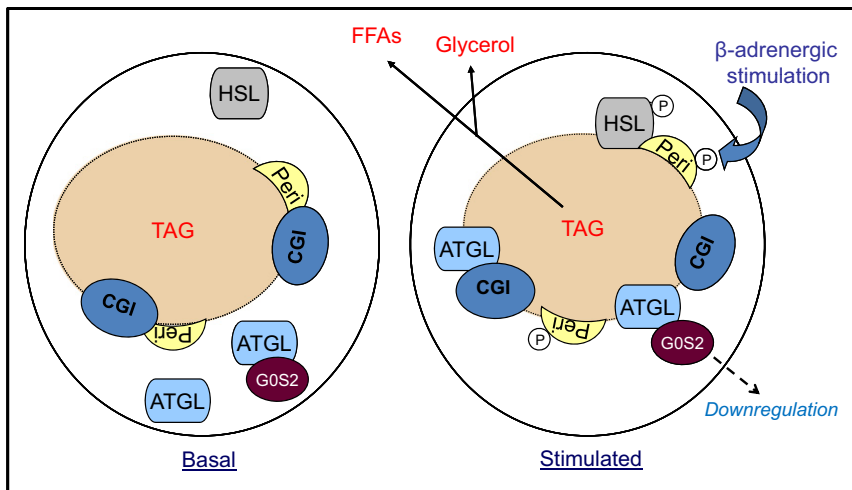


Figure 7. Model for the Regulation of Adipose Lipolysis by G0S2

Under basal conditions when the lipolytic rate is very low, ATGL is mostly localized in ER-related membranes in the cytoplasm. At least a small fraction of ATGL is in complex with G0S2. Upon β -adrenergic stimulation, PKA activation results in phosphorylation of perilipin A at multiple sites. Consequently, ATGL, both G0S2-bound and -unbound form, undergoes translocation onto lipid droplets. Translocation of unbound ATGL along with HSL leads to acute activation of TAG hydrolysis. Prolonged β -adrenergic stimulation subsequently downregulates protein level of G0S2, thereby releasing more ATGL for sustained lipolysis.

phosphorylation event plays any role in the redistribution of ATGL to lipid droplets. Also worth mentioning is a mild accumulation of ATGL and G0S2 in lipid droplets induced by insulin treatment of adipocytes. The precise signaling mechanisms and functional relevance of this observation are currently unknown. We speculate that ATGL, some of which is in the form of ATGL/G0S2 complex, may move onto lipid droplets as a feedback response to lipolytic inhibition or/and lipogenic stimulation elicited by insulin. Prolonged insulin treatment is able to downregulate ATGL expression, thereby reversing this process.

As revealed by coimmunoprecipitation, the interaction between ATGL and G0S2 was not subject to regulation by isoproterenol. Based upon this observation, we speculate that at least a small fraction of ATGL is constantly in complex with G0S2, both in the basal state and during the acute stage of lipolytic stimulation. Although G0S2-bound ATGL is not fully active, it is conceivable that not all ATGL is in association with G0S2, and isoproterenol-stimulated translocation of this free fraction would still allow profound activation of lipolysis (Figure 7). Two lines of evidence that we obtained are supportive of this hypothesis. First, G0S2 underwent similar translocation from cytoplasm to lipid droplets upon isoproterenol treatment. This redistribution was abolished by the knockdown of ATGL, indicating that G0S2 is piggybacked onto lipid droplets by ATGL. The result is consistent with our other finding that the G0S2 binding does not involve the lipid-binding hydrophobic domain of ATGL, allowing simultaneous association of ATGL to G0S2 and lipid droplets. Second, through knockdown and overexpression of G0S2, thereby altering the ratio between free ATGL and G0S2-bound ATGL, we were able to accordingly alter the lipolytic rates in adipocytes.

G0S2 was previously shown to be localized to the endoplasmic reticulum (ER) when expressed in HEK293 cells as well as 3T3-L1 preadipocytes (Zandbergen et al., 2005). ATGL, on the other hand, was found to be tightly associated with membranes when not localized to lipid droplets in HeLa cells (Soni et al., 2009). Therefore, it is possible that, in adipocytes, both G0S2 and ATGL also occur in association with an ER-related membrane compartment, from which they are recruited onto lipid droplets upon adrenergic stimulation. In this regard,

it would be interesting to determine whether coatmer protein I (COPI) complex, the membrane-trafficking machinery responsible for delivering ATGL to lipid droplets in nonadipocytes (Beller et al., 2008; Soni et al., 2009), is also employed for lipid droplet recruitment of ATGL and G0S2 in adipocytes.

Lastly, we found that G0S2 expression was significantly reduced in WAT of *db/db* mice and high-fat-fed wild-type mice. Because obesity is associated with insulin resistance in peripheral tissues, we speculate that impaired insulin sensitivity of adipocytes may lead to the decreased expression of G0S2. It is also possible that increased production of $\text{TNF}\alpha$ by WAT during obesity plays a role in downregulating G0S2 expression, considering that G0S2 level was diminished in adipocytes upon $\text{TNF}\alpha$ treatment (Figure 1D). Moreover, elevated basal lipolytic capacity of adipocytes is known to contribute to increased plasma FFA levels in human obesity (Boden and Shulman, 2002; Guilherme et al., 2008; Watt and Steinberg, 2007) and thus may represent an important risk factor for the development of insulin resistance and type 2 diabetes. Accordingly, further studies will be undertaken to investigate whether expression of G0S2 is also decreased in obese human. If so, it would be important to determine whether a reduced level of G0S2 contributes to the elevated lipolysis associated with obesity.

EXPERIMENTAL PROCEDURES

Production and Purification of Bacterially Expressed G0S2

The full-length mouse G0S2 cDNA was subcloned by standard PCR into pET41a MBP vector (Lu et al., 2008) to produce the protein fused with MBP at the N-terminal end with the TEV cleavage site. For tag-free protein purification, G0S2 was overexpressed in *Escherichia coli* BL21-Gold (Novagen) with induction of 0.5 mM IPTG at an A600 of 0.8–1.0 at 37°C and harvested after culturing for an additional 4–6 hr. The cells were lysed by sonication, and the expressed MBP-fusion proteins were isolated in the presence of 0.6 M NaCl to prevent nonspecific binding to bacterial DNA. G0S2 was released by TEV digestion from amylose magnetic beads (New England Biolabs) after overnight incubation at 4°C and further purified by ion exchange chromatography (Mono-S FPLC). The purified protein was estimated to be at least 98% pure as judged by staining with Coomassie brilliant blue on an 8%–25% gradient SDS-polyacrylamide gel. Fractions were pooled; concentrations were measured by UV absorption and dialyzed into PBS buffer containing 0.25 M sucrose, 1 mM EDTA, and 1 mM DTT.

siRNA-Mediated Knockdown

The following double-stranded stealth siRNA oligonucleotides (Invitrogen) were used: set 1 for mouse G0S2, sense 5'-CAUGCUGUUUCAAGGUGCCA CCGAA-3', antisense 5'-UUCGGUGGCACCUUGAAACAGCAUG-3'; set 2 for mouse G0S2, sense 5'-CACCGAAUCCAGAACUGACCCUACA-3', antisense 5'-UGUAGGGUCAGUUCUGGUAUUCGGUG-3'; human ATGL, set of three validated siRNA oligonucleotides (cat# 1299003); mouse ATGL, set of three validated oligonucleotides (cat# 1320003). Control oligonucleotides with comparable GC content were also from Invitrogen.

For ATGL knockdown in HeLa cells, total 100 pmol of mixed oligonucleotides, 33 pmol of each of the three sets, were transfected into HeLa cells plated in 6-well dishes using Lipofectamine 2000. For ATGL and G0S2 knockdown in 3T3-L1 adipocytes, 4 nmol of mixed oligonucleotides, 2 nmol of each of the three sets, were delivered into cells via electroporation using BioRad Gene Pulser II at 950 μ F and 160V, as described previously (Chen et al., 2007). After 3 days of incubation, cells were processed for designated assays.

Adenoviral Infection of Adipocytes and Adipose Tissue Explants

Recombinant adenovirus containing murine G0S2 cDNA under the control of a CMV promoter (Ad-G0S2) was custom generated by Vector Biolabs. A CMV null virus (Ad null) was also obtained for use in control experiments. Infection of differentiated adipocytes and adipose tissue explants was performed by using a previously published method (Greenberg et al., 2003) with minor modifications. For infection of 3T3-L1 adipocytes, Ad-G0S2 or Ad null were diluted to two concentrations (10^7 and 10^8 pfu/ml) in DMEM, 2% FBS, and 5.0 μ g/ml polybrene and preincubated for 45 min at room temperature. Adipocytes in 6-well dishes were washed once with PBS, and 1.2 ml of preincubated virus mix was added to each well. Cells were centrifuged at 800 \times g for 1 hr at room temperature followed by incubation at 37°C. Fresh growth medium (1.0 ml/well) was added after 4 hr, and cells were incubated for 48–72 hr before use. For infection of adipose tissue explants, gonadal fat pads (~25 mg) freshly isolated from 20-week-old C57BL6 female mice were washed with PBS and then incubated in a microcentrifuge tube containing 150 μ l of virus mix (7×10^8 pfu/ml) for 45 min at room temperature. Following centrifugation at 800 \times g for 1 hr at room temperature, explants along with virus mix were transferred to a 24-well dish and incubated at 37°C. Fresh growth medium (0.5 ml/well) was added after 4 hr, and explants were incubated for 48 hr before use.

Lipid Droplet Fractionation

Lipid droplets were isolated from 3T3-L1 adipocytes as describe previously (Brasaemle and Wolins, 2006). In brief, cells were collected in ice-cold PBS followed by centrifugation for 10 min at 1000 \times g, 4°C. Cell pellets were resuspended in HLM buffer (20 mM Tris-Cl [pH 7.4], 1 mM, 0.5 mM EDTA, 10 mM sodium fluoride, and protease inhibitors) and homogenized by 10 gentle strokes with a hand-driven pestle. The homogenates were centrifuged for 10 min at 1000 \times g, 4°C. The supernatant was collected, and the floating lipid layer was transferred into a separate ultracentrifugation tube. One-third volume of ice-cold HLM containing 60% sucrose (final 20% sucrose) was added, and lipid droplets were mixed thoroughly by gentle pipetting. The mixture was then overloaded sequentially with HLM containing 5% sucrose and HLM containing no sucrose. After centrifugation for 30 min at 28,000 \times g, 4°C, the floating lipid droplet fraction was collected by using a Beckman tube slicer. Equal volume of 10% SDS was added, and proteins associated with lipid droplets were solubilized by incubation for 2 hr at 37°C in a sonicating water bath.

Assay for TAG Hydrolase Activity

For assays with HeLa cell extracts, cells in 10 cm dishes were washed twice in ice-cold PBS and then disrupted on ice by passing 10 times through a 22G needle in 0.5 ml of cell extraction buffer (0.25 M sucrose, 1 mM EDTA, 1 mM DTT, and protease inhibitors [1 mini tablet per 7 ml of volume]). For assays with WAT and BAT, epididymal and interscapular fat pads were homogenized in cell extraction buffer by a drill press as described above. The cell and tissue extracts were clarified by centrifugation at 1000 \times g for 15 min. The TAG hydrolase activity against 3 H-labeled triolein was measured as described previously (Lass et al., 2006; Zimmermann et al., 2004) by mixing 0.1 ml of extracts with 0.1 ml of substrate solution. For assays using in vitro transcription/translation products, a total of 35 μ l of reaction mixture was prediluted

with 65 μ l of cell extraction buffer. The resulting 0.1 ml of reaction mixture was then combined with 0.1 ml of substrate solution in the TAG hydrolase activity measurement.

Lipolysis Assay and Measurement of Intracellular TAG Content

Lipolysis was measured as the rate of glycerol and free fatty acid release. In brief, adipocytes or gonadal WAT explants in 12-well dishes were incubated in 1 ml of assay buffer in the presence or absence of 1 μ M isoproterenol. Aliquots of assay buffer were collected over a 30 min–2 hr period. The amounts of glycerol and FFAs released were determined by using a lipolysis assay kit (Zenbio) according to the manufacturer's instructions. Lysates were then prepared from the remaining cells, and protein concentrations in the lysates were used to normalize the lipolytic signals.

Triglyceride accumulation was measured using a triglyceride assay kit (Zenbio). In brief, at the indicated time after oleic acid treatment, HeLa cells were washed and lysed in provided lysis buffer. Then the triglyceride assay reagents were added according to the manufacturer's instructions. The optical density of the solution was measured at 540 nm using a spectrophotometer plate reader. TAG concentration was calculated from a standard curve for each assay, and data is normalized to total cellular protein.

SUPPLEMENTAL INFORMATION

Supplemental Information includes Supplemental Experimental Procedures and four figures and can be found with this article online at doi:10.1016/j.cmet.2010.02.003.

ACKNOWLEDGMENTS

We thank Drs. Carole Sztalryd, Matthew J. Brady, Xiaowei Chen, Alan Cheng, and William V. Everson for reviewing the manuscript and helpful discussions. We also thank Dr. Say Viengchareun for excellent technical advice. The work was supported by a NIH grant DK 078742 and a Center of Biomedical Research Excellence pilot grant from the University of Kentucky (5P20 RR0202171) to J.L. and NIH grants RR015592 and DK077632 to E.J.S.

Received: August 17, 2009

Revised: December 10, 2009

Accepted: February 5, 2010

Published: March 2, 2010

REFERENCES

- Ahmadian, M., Duncan, R.E., Varady, K.A., Frasson, D., Hellerstein, M.K., Birkenfeld, A.L., Samuel, V.T., Shulman, G.I., Wang, Y., Kang, C., and Sul, H.S. (2009). Adipose overexpression of desnutrin promotes fatty acid use and attenuates diet-induced obesity. *Diabetes* 58, 855–866.
- Beller, M., Sztalryd, C., Southall, N., Bell, M., Jäckle, H., Auld, D.S., and Oliver, B. (2008). COPI complex is a regulator of lipid homeostasis. *PLoS Biol.* 6, e292.
- Bezaire, V., Mairal, A., Ribet, C., Lefort, C., Girousse, A., Jocken, J., Laurencikene, J., Anesia, R., Rodriguez, A.M., Ryden, M., et al. (2009). Contribution of adipose triglyceride lipase and hormone-sensitive lipase to lipolysis in hMADS adipocytes. *J. Biol. Chem.* 284, 18282–18291.
- Boden, G., and Shulman, G.I. (2002). Free fatty acids in obesity and type 2 diabetes: defining their role in the development of insulin resistance and beta-cell dysfunction. *Eur. J. Clin. Invest.* 32 (Suppl 3), 14–23.
- Brasaemle, D.L., and Wolins, N.E. (2006). Isolation of lipid droplets from cells by density gradient centrifugation. *Curr. Protoc. Cell Biol.* Unit 3, 15.
- Chen, X.W., Leto, D., Chiang, S.H., Wang, Q., and Saltiel, A.R. (2007). Activation of RalA is required for insulin-stimulated Glut4 trafficking to the plasma membrane via the exocyst and the motor protein Myo1c. *Dev. Cell* 13, 391–404.
- Chung, C., Doll, J.A., Gattu, A.K., Shugrue, C., Cornwell, M., Fitchev, P., and Crawford, S.E. (2008). Anti-angiogenic pigment epithelium-derived factor regulates hepatocyte triglyceride content through adipose triglyceride lipase (ATGL). *J. Hepatol.* 48, 471–478.

- Dessen, A., Tang, J., Schmidt, H., Stahl, M., Clark, J.D., Seehra, J., and Somers, W.S. (1999). Crystal structure of human cytosolic phospholipase A2 reveals a novel topology and catalytic mechanism. *Cell* 97, 349–360.
- Duncan, R.E., Ahmadian, M., Jaworski, K., Sarkadi-Nagy, E., and Sul, H.S. (2007). Regulation of lipolysis in adipocytes. *Annu. Rev. Nutr.* 27, 79–101.
- Egan, J.J., Greenberg, A.S., Chang, M.K., Wek, S.A., Moos, M.C., Jr., and Londos, C. (1992). Mechanism of hormone-stimulated lipolysis in adipocytes: translocation of hormone-sensitive lipase to the lipid storage droplet. *Proc. Natl. Acad. Sci. USA* 89, 8537–8541.
- Fischer, J., Lefèvre, C., Morava, E., Mussini, J.M., Laforêt, P., Negre-Salvayre, A., Lathrop, M., and Salvayre, R. (2007). The gene encoding adipose triglyceride lipase (PNPLA2) is mutated in neutral lipid storage disease with myopathy. *Nat. Genet.* 39, 28–30.
- Granneman, J.G., Moore, H.P., Granneman, R.L., Greenberg, A.S., Obin, M.S., and Zhu, Z. (2007). Analysis of lipolytic protein trafficking and interactions in adipocytes. *J. Biol. Chem.* 282, 5726–5735.
- Greenberg, C.C., Meredith, K.N., Yan, L., and Brady, M.J. (2003). Protein targeting to glycogen overexpression results in the specific enhancement of glycogen storage in 3T3-L1 adipocytes. *J. Biol. Chem.* 278, 30835–30842.
- Guilherme, A., Virbasius, J.V., Puri, V., and Czech, M.P. (2008). Adipocyte dysfunctions linking obesity to insulin resistance and type 2 diabetes. *Nat. Rev. Mol. Cell Biol.* 9, 367–377.
- Haemmerle, G., Lass, A., Zimmermann, R., Gorkiewicz, G., Meyer, C., Rozman, J., Heldmaier, G., Maier, R., Theussl, C., Eder, S., et al. (2006). Defective lipolysis and altered energy metabolism in mice lacking adipose triglyceride lipase. *Science* 312, 734–737.
- Huijsman, E., van de Par, C., Economou, C., van der Poel, C., Lynch, G.S., Schoiswohl, G., Haemmerle, G., Zechner, R., and Watt, M.J. (2009). Adipose triacylglycerol lipase deletion alters whole body energy metabolism and impairs exercise performance in mice. *Am. J. Physiol. Endocrinol. Metab.* 297, E505–E513.
- Jenkins, C.M., Mancuso, D.J., Yan, W., Sims, H.F., Gibson, B., and Gross, R.W. (2004). Identification, cloning, expression, and purification of three novel human calcium-independent phospholipase A2 family members possessing triacylglycerol lipase and acylglycerol transacylase activities. *J. Biol. Chem.* 279, 48968–48975.
- Kershaw, E.E., Hamm, J.K., Verhagen, L.A., Peroni, O., Katic, M., and Flier, J.S. (2006). Adipose triglyceride lipase: function, regulation by insulin, and comparison with adiponutrin. *Diabetes* 55, 148–157.
- Kobayashi, K., Inoguchi, T., Maeda, Y., Nakashima, N., Kuwano, A., Eto, E., Ueno, N., Sasaki, S., Sawada, F., Fujii, M., et al. (2008). The lack of the C-terminal domain of adipose triglyceride lipase causes neutral lipid storage disease through impaired interactions with lipid droplets. *J. Clin. Endocrinol. Metab.* 93, 2877–2884.
- Langin, D., Dicker, A., Tavernier, G., Hoffstedt, J., Mairal, A., Rydén, M., Arner, E., Sicard, A., Jenkins, C.M., Viguier, N., et al. (2005). Adipocyte lipases and defect of lipolysis in human obesity. *Diabetes* 54, 3190–3197.
- Lass, A., Zimmermann, R., Haemmerle, G., Riederer, M., Schoiswohl, G., Schweiger, M., Kienesberger, P., Strauss, J.G., Gorkiewicz, G., and Zechner, R. (2006). Adipose triglyceride lipase-mediated lipolysis of cellular fat stores is activated by CGI-58 and defective in Chanarin-Dorfman Syndrome. *Cell Metab.* 3, 309–319.
- Lefèvre, C., Jobard, F., Caux, F., Bouadjar, B., Karaduman, A., Heilig, R., Lakhdar, H., Wollenberg, A., Verret, J.L., Weissenbach, J., et al. (2001). Mutations in CGI-58, the gene encoding a new protein of the esterase/lipase/thioesterase subfamily, in Chanarin-Dorfman syndrome. *Am. J. Hum. Genet.* 69, 1002–1012.
- Lu, P., Rha, G.B., Melikishvili, M., Wu, G., Adkins, B.C., Fried, M.G., and Chi, Y.I. (2008). Structural basis of natural promoter recognition by a unique nuclear receptor, HNF4alpha. *Diabetes gene product. J. Biol. Chem.* 283, 33685–33697.
- Ma, L., Robinson, L.N., and Towle, H.C. (2006). ChREBP^{Mlx} is the principal mediator of glucose-induced gene expression in the liver. *J. Biol. Chem.* 281, 28721–28730.
- Martin, S., and Parton, R.G. (2006). Lipid droplets: a unified view of a dynamic organelle. *Nat. Rev. Mol. Cell Biol.* 7, 373–378.
- Miyoshi, H., Perfield, J.W., II, Souza, S.C., Shen, W.J., Zhang, H.H., Stancheva, Z.S., Kraemer, F.B., Obin, M.S., and Greenberg, A.S. (2007). Control of adipose triglyceride lipase action by serine 517 of perilipin A globally regulates protein kinase A-stimulated lipolysis in adipocytes. *J. Biol. Chem.* 282, 996–1002.
- Notari, L., Baladron, V., Aroca-Aguilar, J.D., Balko, N., Heredia, R., Meyer, C., Notario, P.M., Saravanamuthu, S., Nueda, M.L., Sanchez-Sanchez, F., et al. (2006). Identification of a lipase-linked cell membrane receptor for pigment epithelium-derived factor. *J. Biol. Chem.* 281, 38022–38037.
- Parikh, H., Carlsson, E., Chutkow, W.A., Johansson, L.E., Storgaard, H., Poulsen, P., Saxena, R., Ladd, C., Schulze, P.C., Mazzini, M.J., et al. (2007). TXNIP regulates peripheral glucose metabolism in humans. *PLoS Med.* 4, e158.
- Raben, D.M., and Baldassare, J.J. (2005). A new lipase in regulating lipid mobilization: hormone-sensitive lipase is not alone. *Trends Endocrinol. Metab.* 16, 35–36.
- Russell, L., and Forsdyke, D.R. (1991). A human putative lymphocyte G0/G1 switch gene containing a CpG-rich island encodes a small basic protein with the potential to be phosphorylated. *DNA Cell Biol.* 10, 581–591.
- Rydel, T.J., Williams, J.M., Krieger, E., Moshiri, F., Stallings, W.C., Brown, S.M., Pershing, J.C., Purcell, J.P., and Alibhai, M.F. (2003). The crystal structure, mutagenesis, and activity studies reveal that patatin is a lipid acyl hydrolase with a Ser-Asp catalytic dyad. *Biochemistry* 42, 6696–6708.
- Rydén, M., Jocken, J., van Harmelen, V., Dicker, A., Hoffstedt, J., Wirén, M., Blomqvist, L., Mairal, A., Langin, D., Blaak, E., and Arner, P. (2007). Comparative studies of the role of hormone-sensitive lipase and adipose triglyceride lipase in human fat cell lipolysis. *Am. J. Physiol. Endocrinol. Metab.* 292, E1847–E1855.
- Schweiger, M., Schoiswohl, G., Lass, A., Radner, F.P., Haemmerle, G., Malli, R., Graier, W., Cornaciu, I., Oberer, M., Salvayre, R., et al. (2008). The C-terminal region of human adipose triglyceride lipase affects enzyme activity and lipid droplet binding. *J. Biol. Chem.* 283, 17211–17220.
- Smirnova, E., Goldberg, E.B., Makarova, K.S., Lin, L., Brown, W.J., and Jackson, C.L. (2006). ATGL has a key role in lipid droplet/adiposome degradation in mammalian cells. *EMBO Rep.* 7, 106–113.
- Soni, K.G., Mardones, G.A., Sougrat, R., Smirnova, E., Jackson, C.L., and Bonifacio, J.S. (2009). Coatamer-dependent protein delivery to lipid droplets. *J. Cell Sci.* 122, 1834–1841.
- Sztalryd, C., Xu, G., Dorward, H., Tansey, J.T., Contreras, J.A., Kimmel, A.R., and Londos, C. (2003). Perilipin A is essential for the translocation of hormone-sensitive lipase during lipolytic activation. *J. Cell Biol.* 161, 1093–1103.
- Villena, J.A., Roy, S., Sarkadi-Nagy, E., Kim, K.H., and Sul, H.S. (2004). Desnutrin, an adipocyte gene encoding a novel patatin domain-containing protein, is induced by fasting and glucocorticoids: ectopic expression of desnutrin increases triglyceride hydrolysis. *J. Biol. Chem.* 279, 47066–47075.
- Watt, M.J., and Steinberg, G.R. (2007). Pathways involved in lipid-induced insulin resistance in obesity. *Future Medicine* 2, 659–667.
- Watt, M.J., and Steinberg, G.R. (2008). Regulation and function of triacylglycerol lipases in cellular metabolism. *Biochem. J.* 414, 313–325.
- Zandbergen, F., Mandard, S., Escher, P., Tan, N.S., Patsouris, D., Jatke, T., Rojas-Caro, S., Madore, S., Wahli, W., Tafuri, S., et al. (2005). The G0/G1 switch gene 2 is a novel PPAR target gene. *Biochem. J.* 392, 313–324.
- Zechner, R., Kienesberger, P.C., Haemmerle, G., Zimmermann, R., and Lass, A. (2009). Adipose triglyceride lipase and the lipolytic catabolism of cellular fat stores. *J. Lipid Res.* 50, 3–21.
- Zimmermann, R., Strauss, J.G., Haemmerle, G., Schoiswohl, G., Birner-Gruenberger, R., Riederer, M., Lass, A., Neuberger, G., Eisenhaber, F., Hermetter, A., and Zechner, R. (2004). Fat mobilization in adipose tissue is promoted by adipose triglyceride lipase. *Science* 306, 1383–1386.
- Zimmermann, R., Lass, A., Haemmerle, G., and Zechner, R. (2009). Fate of fat: the role of adipose triglyceride lipase in lipolysis. *Biochim. Biophys. Acta* 1791, 494–500.